Available online at www.sciencedirect.com
SCIENCE DIRECT®
Applied Surface Science 247 (2005) 423–428
applied surface science
www.elsevier.com/locate/apsusc

Morphological and structural characterization of CrO_2/Cr_2O_3 films grown by Laser-CVD

P.M. Sousa [a], A.J. Silvestre [b], N. Popovici [a], O. Conde [a,*]

[a] *Departamento de Física, Universidade de Lisboa, Ed. C8, Campo Grande, 1749-016 Lisboa, Portugal*
[b] *Instituto Superior de Engenharia de Lisboa, R. Conselheiro Emídio Navarra, 1950-062 Lisboa, Portugal*

Available online 16 February 2005

Abstract

This work reports on the synthesis of chromium (III, IV) oxides films by KrF laser-assisted CVD. Films were deposited onto sapphire substrates at room temperature by the photodissociation of $Cr(CO)_6$ in dynamic atmospheres containing oxygen and argon. A study of the processing parameters has shown that partial pressure ratio of O_2 to $Cr(CO)_6$ and laser fluence are the prominent parameters that have to be accurately controlled in order to co-deposit both the crystalline oxide phases. Films consistent with such a two-phase system were synthesised for a laser fluence of 75 mJ cm^{-2} and a partial pressure ratio of about 1.

PACS: 81.15.Fg; 81.15.Kk; 81.05.Je

Keywords: Laser-assisted CVD; Photodissociation; CrO_2/Cr_2O_3 two-phase system

1. Introduction

Chromium oxide thin films are of great interest due to their wide variety of technological applications. The most stable phase is the insulating antiferromagnetic Cr_2O_3. This oxide has several applications, for instance, in catalysis [1] and solar thermal energy collectors [2]. Currently, low-reflective Cr_2O_3/Cr films are widely used as black matrix films in liquid crystal displays [2]. Cr_2O_3 films are also used as protective films because of their good chemical and wear resistance, and low friction coefficient [3]. In contrast, chromium dioxide (CrO_2) is strongly ferromagnetic at room temperature ($T_C = 393$ K) and has a half-metallic band structure fully spin-polarised at the Fermi level [4–7], making it extremely attractive for use in the magnetoelectronic devices. Furthermore, Cr_2O_3/CrO_2 biphasic films show remarkable magnetoresistance due to intergrain tunnelling between high spin polarized crystals [8,9]. However, the synthesis of chromium (III, IV) oxide mixtures at temperatures compatible with semiconductor proces-

* Corresponding author. Tel.: +351 21 7500035; fax: +351 21 7500977.
E-mail address: oconde@fc.ul.pt (O. Conde).

0169-4332/$ – see front matter © 2005 Elsevier B.V. All rights reserved.
doi:10.1016/j.apsusc.2005.01.061

Table 1
LCVD experimental conditions used to deposit chromium oxide films

Experimental parameters	Values	Estimated parameters	Values
Beam energy (E) (mJ)	4.1–15.6	Fluence at the substrate (F) (mJ cm^{-2})	50–190
Spot area (S) (mm^2)	8.2	$Cr(CO)_6$ flux (Φ_{Cr}) (sccm)	1.1–1.3
$Cr(CO)_6$ cell temperature (T_{cell}) (°C)	19–22	$Cr(CO)_6$ partial pressure (p_{Cr}) (Pa)	0.7–2.3
O_2 carrier flux (Φ_{O_2}) (sccm)	1–10	O_2 partial pressure (p_{O_2}) (Pa)	0.0–8.0
Ar flux (Φ_{Ar}) (sccm)	50	Ar partial pressure (p_{Ar}) (Pa)	40.1–48.8
Deposition time (t_{dep}) (min)	240–360		

sing has been a difficult task due to the metastability of CrO_2 which easily decomposes into the insulating antiferromagnetic Cr_2O_3 phase. Therefore, there is a continuous search for the deposition methods that allow the growth of these films at low temperatures.

Laser-assisted CVD is a selective area deposition technique which has the potential to meet the requirements stated above. In a few previous studies, Dowben et al. [10–13] carried out the photolytic decomposition of $Cr(CO)_6$ by nitrogen laser radiation ($\lambda = 337$ nm) in static conditions, having shown the synthesis of films containing both Cr_2O_3 and CrO_2 phases. Looking for a better efficiency of the deposition process, it seems to be advantageous to explore dynamic atmospheres and to use other UV wavelengths for which $Cr(CO)_6$ absorption cross section is much higher than for the nitrogen laser, e.g. KrF laser radiation ($\lambda = 248$ nm) [14,15].

In this paper, we present results on the synthesis of chromium (III, IV) oxide films produced by KrF laser-assisted CVD. Films were grown onto Al_2O_3 (0 0 0 1) substrates at room temperature by photodissociation of $Cr(CO)_6$ in dynamic atmospheres containing O_2 and Ar.

2. Experimental details

The experimental apparatus used for the experiments consists of a KrF excimer laser, a stainless steel HV chamber, a HV pumping system and a gas system for delivering the reactants to the reaction chamber. The KrF laser ($\lambda = 248$ nm, $\tau = 30$ ns) has a beam dimension of 24×12 mm^2. The laser beam impinges on the substrate at a perpendicular incidence and by using an adequate optical system, it is possible to control the beam spot size and thus the fluence at the substrate surface. The laser fluences reported in Table 1 have been evaluated taking into account both the beam energy loss on the optical components and the energy loss due to the absorption by the reactant gas mixture. Prior to any deposition experiment, the reactor was always evacuated to a base pressure lower than 5×10^{-4} Pa. All the deposition experiments were conducted in dynamic regime. Ar was used as a buffer gas and to flash the inner face of the chamber window used for transmission of the laser beam.

Chromium hexacarbonyl powder was sublimated in a controlled temperature stainless steel cell connected to the LCVD reactor. The $Cr(CO)_6$ vapour pressure is given by the following equation [9]: $\log_{10}P$ (Pa) = 12.75–3285/T (K). Oxygen was used as carrier gas except in the experiments carried out in a non-oxidant atmosphere where it was replaced by argon. The partial pressures of $Cr(CO)_6$, O_2 and Ar inside the reactor are settled by the cell temperature, the flux of the carrier gas, the flux of Ar and the total working pressure, assuming a viscous flow regime between the cell and the reactor. The chromium oxide films were grown at room temperature on Al_2O_3 (0 0 0 1) substrates for a laser pulse repetition rate of 5 Hz and total pressure $P_T = 50$ Pa. The overall experimental parameters are summarised in Table 1.

In order to study the chromium oxide phases synthesised as a function of laser fluence and partial pressure ratio of O_2 and $Cr(CO)_6$, structural analysis of the as-deposited films was carried out by X-ray diffraction with Cu Kα radiation and by micro-Raman spectroscopy using the 514.5 nm excitation line of an Ar^+ laser. The morphology and microstructure of the films were analysed by optical microscopy (OM) and scanning electron microscopy (SEM), and their thickness measured by stylus profilometry.

3. Results and discussion

3.1. Surface morphology and microstructure

The as-deposited films present good adherence and are approximately rectangular in shape following the laser beam profile. OM observations revealed that they are quite homogeneous and exhibit a colour varying between greenish and nearly black, depending on the processing parameters used on their synthesis. Since Cr_2O_3 has a characteristic green colour while CrO_2 is black, film colour can be used as first control to infer the presence of chromium dioxide in the deposited material. Films produced with partial pressure ratio $p_{O_2}/p_{Cr} = 1$ tend to be darker otherwise the greenish colouration tends to be dominant. Also the microstructure of the films may be related with both the chromium oxide phases. As documented in literature [16], films of Cr_2O_3 often consist of spheroid particles whereas CrO_2 usually appears as rod-shaped particles. SEM analysis of our samples shows a microstructure consisting mainly of granular and randomly oriented rod-shaped particles, the latter prevailing in the darker films synthesised with $p_{O_2}/p_{Cr} = 1$ (Fig. 1). As it will be discussed hereafter, the structural analysis of the samples strongly supports that films produced with $p_{O_2}/p_{Cr} = 1$ are those with the higher content of CrO_2.

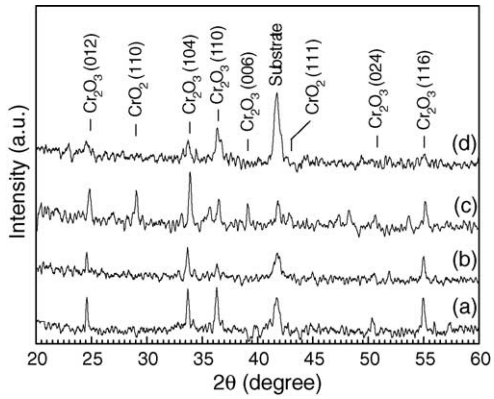

Fig. 2. XRD patterns of films deposited during 4 h at total pressure of 50 Pa, $F = 75$ mJ cm^{-2} and various p_{O_2}/p_{Cr} ratios: (a) $p_{O_2}/p_{Cr} = 0$; (b) $p_{O_2}/p_{Cr} = 0.7$; (c) $p_{O_2}/p_{Cr} = 1$; and (d) $p_{O_2}/p_{Cr} = 4.4$.

3.2. Structural analysis

3.2.1. Effect of gas phase composition

Fig. 2 shows X-ray diffraction patterns of films deposited during 4 h with $F = 75$ mJ cm^{-2} and p_{O_2}/p_{Cr} ratios ranging from 0 to 4.4. For films grown at $p_{O_2}/p_{Cr} < 1$ (Fig. 2a and b), only the Cr_2O_3 crystallographic planes match the diffractograms and no traces of crystalline CrO_2 phase were observed. Also the film deposited with $p_{O_2}/p_{Cr} > 1$ (Fig. 2d)

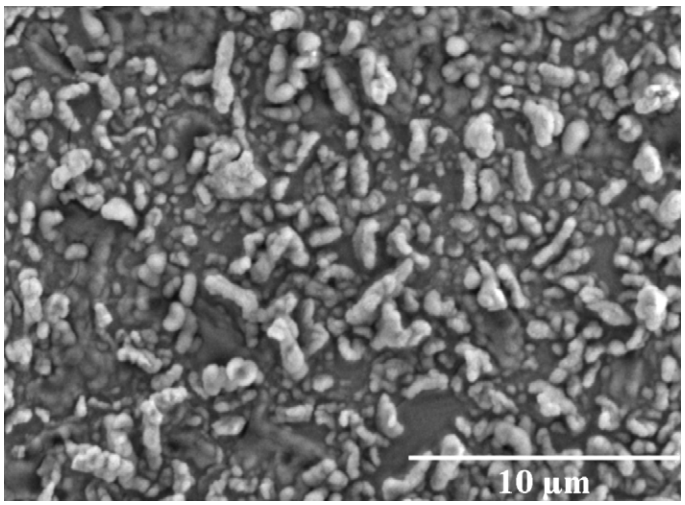

Fig. 1. SEM image of a film deposited during 4 h with the following deposition parameters: $P_T = 50$ Pa, $\Phi_{Cr} = 1$ sccm, $\Phi_{O_2} = 1$ sccm, $\Phi_{Ar} = 50$ sccm and $F = 75$ mJ cm^{-2}.

shows no evidence of chromium dioxide deposition. The formation of both the polycrystalline Cr_2O_3 and CrO_2 phases was achieved in samples grown with $p_{O_2}/p_{Cr} = 1$ (Fig. 2c). In this diffractogram, both the characteristic diffraction peaks of Cr_2O_3 and the (1 1 0) and (1 1 1) diffraction lines of CrO_2 can be clearly seen. Although the role of oxygen on the chemical reaction that leads to the co-deposition of both chromium oxide phases by photodecomposition of $Cr(CO)_6$ is not completely understood, our results show that oxygen is absolutely necessary to synthesise CrO_2 but not to achieve Cr_2O_3 deposition. In fact, the latter phase can be grown without oxygen (Fig. 2a) as a result of the recombination of Cr with the free oxygen released from the decomposition of $Cr(CO)_6$ at low temperature [17,18]. Dowben and co-workers [11,12] have pointed out that the partial pressure of oxygen is the prominent parameter to be controlled in order to tailor the relative amount of Cr_2O_3 and CrO_2 that results from the dissociation of $Cr(CO)_6$, suggesting that an increase of the p_{O_2}/p_{Cr} ratio should allow to improve the formation of CrO_2. Our results show that the co-deposition of both polycrystalline oxide phases is only obtained when the precursors partial pressure ratio is close to unity. On the other hand, the observed broadening of the Cr_2O_3 diffraction peaks when p_{O_2}/p_{Cr} increases suggests that higher p_{O_2}/p_{Cr} ratios induce some degree of amorphisation of this phase, similarly to what has been observed in CVD processes of Cr_2O_3 using the same precursors as in the present work [19].

3.2.2. *Effect of laser fluence*

Besides partial pressures ratio, laser fluence also plays an important role on the phase composition of the deposited material. When absorbing two photons at 248 nm, an isolated $Cr(CO)_6$ molecule should decompose to Cr and 6CO with a quantum yield given in literature as ~1 [20]. By reacting with O_2, the photodissociated Cr species would give rise to CrO_2. However, the mechanism by which the photodissociation of $Cr(CO)_6$ may lead to chromium dioxide is quite complex and still not clear. A simplified scheme can be drawn as follows: a single 248 nm photon leads to the removal of two carbonyl ligands resulting in $Cr(CO)_4$ formation [14,20,21]. At laser fluence higher than 5 mJ cm^{-2}, a second photon gives rise to secondary photodissociation of $Cr(CO)_4$ into Cr^* and 4CO. Then, the formation of CrO_2 proceeds via the reaction of the excited chromium with oxygen. Surface reactions at the substrate surface such as $2CrO_2 \rightarrow Cr_2O_3 + 1/2O_2$ may occur, the final composition of the deposited material depending on the extension of this reaction. Nevertheless, these features are only true for a very low pressure of $Cr(CO)_6$, for which collisions are absent. In systems where collisions play an important role, the statistical fragmentation processes that follow the initial photodissociation event may be inhibited by collision vibrational relaxation of the photoproducts. As we aim at achieving co-deposition of both Cr_2O_3 and CrO_2 at a significant growth rate, higher pressures are required and, consequently, higher laser fluences should be used. For the range of pressures given in this work,

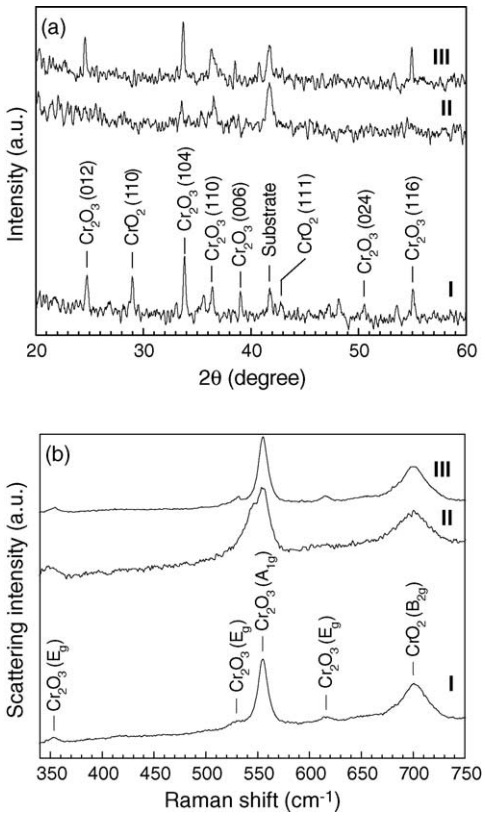

Fig. 3. (a) XRD patterns and (b) micro-Raman spectra of films deposited during 4 h with different fluences. Deposition parameters: $P_T = 50$ Pa, $\Phi_{Cr} = 1$ sccm, $\Phi_{O_2} = 1$ sccm and $\Phi_{Ar} = 50$ sccm. Film I, $F = 75$ mJ cm^{-2}; film II, $F = 60$ mJ cm^{-2}; film III, $F = 100$ mJ cm^{-2}. Each Raman spectrum was normalised to its Cr_2O_3 A_{1g} peak intensity.

Table 2
Main features of the Cr_2O_3 A_{1g} and CrO_2 B_{2g} Raman bands of films referred to Fig. 3b

Film reference	Band position (cm^{-1})		FWHM (cm^{-1})		Intensity ratio
	Cr_2O_3 (A_{1g})	CrO_2 (B_{2g})	Cr_2O_3 (A_{1g})	CrO_2 (B_{2g})	CrO_2 (B_{2g})/Cr_2O_3 (A_{1g})
Film I	554.9	701.5	11.0	29.5	0.542
Film II	551.5	699.5	24.6	35.7	0.478
Film III	555.1	700.6	10.4	29.6	0.524

chromium oxide deposition was obtained only for the laser fluences higher than 50 mJ cm^{-2}.

Fig. 3 shows X-ray diffraction patterns (Fig. 3a) and micro-Raman spectra (Fig. 3b) of the films deposited during 4 h with $p_{O_2}/p_{Cr} = 1$ and various laser fluences. Each Raman spectrum was normalised to its Cr_2O_3 A_{1g} peak intensity to ease the comparison among the various spectra. As previously described, the XRD pattern of the film grown with $F = 75$ mJ cm^{-2} (Fig. 3a, film I) clearly matches the (1 1 0) and (1 1 1) diffraction planes of CrO_2 as well as the diffraction lines of Cr_2O_3. Confirming the synthesis of chromium (III, IV) oxides, the micro-Raman spectrum recorded over the same sample (Fig. 2b, film I) reveals an intense peak assigned to the B_{2g} mode of CrO_2, at 701.5 cm^{-1} Raman shift, in addition to the symmetric bands of Cr_2O_3 [22,23]. By decreasing the laser fluence, film thickness decreases and a higher degree of amorphisation is induced in the deposited material. In fact, on the XRD pattern of the film synthesised with $F = 60$ mJ cm^{-2} (Fig. 3a, film II), only the (1 0 4) and (1 1 0) diffraction peaks of Cr_2O_3 can be clearly identified and these peaks are broader and less intense than for film I. Concerning the chromium dioxide, the XRD data indicate that either it was not formed at this fluence or it formed with an extremely high level of amorphisation. However, the micro-Raman spectrum of the same film (Fig. 3b, film II) provides evidence that co-deposition of CrO_2 and Cr_2O_3 still occurs at $F = 60$ mJ cm^{-2}; besides the Cr_2O_3 peaks, also the CrO_2 B_{2g} band is present in the Raman spectrum. Table 2 summarises the principle features of the Cr_2O_3 A_{1g} and CrO_2 B_{2g} Raman bands evaluated by fitting the spectra of Fig. 3b with Lorentzian curves. By comparing the data for films I and II, the amorphisation of both the oxides is well observed via the increase of the full-width at half-maximum (FWHM) of the Cr_2O_3 A_{1g} and CrO_2 B_{2g} symmetric modes for film II. Besides amorphisation, a low laser fluence also yields a low relative content of CrO_2 since the intensity ratio I(CrO_2 B_{2g})/I(Cr_2O_3 A_{1g}) for film II is about 12% lower than for film I.

On the other hand, the increase of laser fluence to 100 mJ cm^{-2} favours the deposition of crystalline Cr_2O_3. The FWHM of the band at $\sim$555 cm^{-1} decreases from film I to film III and the Cr_2O_3 E_g bands are better resolved for film III (Fig. 3b). The absence of CrO_2 diffraction lines on pattern III of Fig. 3a may be due to an extended transformation of the initially formed CrO_2 into Cr_2O_3 caused by the heating of the film/substrate during the deposition process at higher laser fluences. Indeed, films processed with $F > 120$ mJ cm^{-2} showed evidence either of surface melting or phase transformation of the sapphire substrate.

From XRD and micro-Raman structural analysis, one can conclude that narrow windows for the laser fluence and p_{O_2}/p_{Cr} ratio, centred respectively at 75 mJ cm^{-2} and 1, have to be used in order to grow

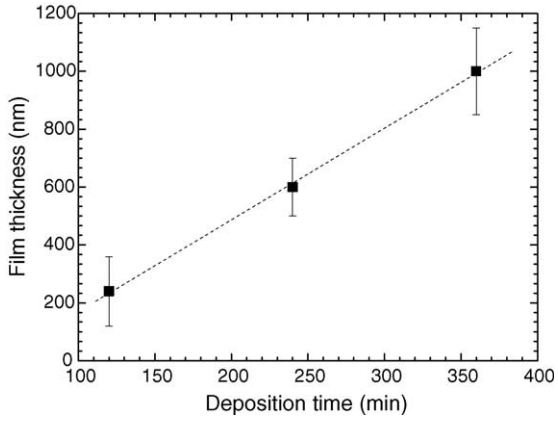

Fig. 4. Film thickness vs. deposition time for chromium (III, IV) oxides films processed with the following parameters: $P_T = 50$ Pa, $\Phi_{Cr} = 1$ sccm, $\Phi_{O_2} = 1$ sccm, $\Phi_{Ar} = 50$ sccm and $F = 75$ mJ cm^{-2}. (■), Experimental data; (- - -), curve fit.

crystalline chromium oxide thin films containing both the CrO_2 and Cr_2O_3 phases.

3.3. Growth rate

Films prepared with the experimental conditions mentioned above present near flat thickness profiles and their thickness increases linearly with the deposition time (Fig. 4), giving an apparent deposition rate of 3.2 nm min^{-1}. The intersection of the straight line with the time axis gives a characteristic time $\Delta t \cong 50$ min, which is very close to the time delay observed experimentally between the instant the laser is turned on and the abrupt change of the sample reflectivity.

4. Conclusion

Films displaying a behaviour consistent with the two-phase system of Cr_2O_3 and CrO_2 oxides were produced by KrF laser photodissociation of $Cr(CO)_6$ in dynamic atmospheres containing oxygen and argon. This technique seems to open an interesting approach to the synthesis of biphasic chromium (III, IV) oxides films at room temperature. It was shown that partial pressures ratio of the precursors and laser fluence are the prominent parameters that have to be accurately controlled in order to co-deposit both the crystalline oxide phases. Biphasic films with both the CrO_2 and Cr_2O_3 phases were grown for laser fluence and p_{O_2}/p_{Cr} ratio values centred at 75 mJ cm^{-2} and 1, respectively. For these films, a deposition rate of 3.2 nm min^{-1} was measured.

Acknowledgement

This work was supported by the EU contract FENIKS: G5RD-CT-2001-00535 and by Fundação para a Ciência e Tecnologia (Portugal) under project ref. POCTI/CTM/41413/01.

References

[1] P.S. Robbert, H. Geisler, C.A. Ventrice, J. van Ek Jr., S. Chaturvedi, J.A. Rodriguez, M. Kuhn, U. Diebold, J. Vac. Sci. Technol., A 16 (1998) 990.
[2] T. Maruyama, H. Akagi, J. Electrochem. Soc. 143 (1996) 1955.
[3] A.L. Ji, W. Wang, G.H. Song, Q.M. Wang, C. Sun, L.S. Wen, Mater. Lett. 58 (2004) 1993.
[4] K.J. Schwartz, J. Phys. F: Met. Phys. 16 (1986) L211.
[5] M.A. Korotin, V.I. Anisimov, D.I. Khomskii, G.A. Sawatzky, Phys. Rev. Lett. 80 (1998) 4305.
[6] R.J. Soulen Jr., J.M. Byers, M.S. Osofsky, B. Nadgorny, T. Ambrose, S.F. Cheng, P.R. Broussard, C.T. Tanaka, J. Nowak, J.S. Moodera, A. Barry, J.M.D. Coey, Science 282 (1998) 85.
[7] Y. Ji, G.J. Strijkers, F.Y. Yang, C.L. Chien, J.M. Byers, A. Anguelouch, G. Xiao, A. Gupta, Phys. Rev. Lett. 86 (2001) 5585.
[8] J.M.D. Coey, A.E. Berkowitz, Ll. Balcells, F.F. Putris, A. Barry, Phys. Rev. Lett. 80 (1998) 3815.
[9] N. Pilet, C. Borca, A. Sokolov, E. Ovtchenkov, Bo Xu, B. Doudin, Mater. Lett. 58 (2004) 2016.
[10] P.A. Dowben, Y.G. Kim, S. Baral-Tosh, G.O. Ramseyer, C. Hwang, M. Onellion, J. Appl. Phys. 67 (1990) 5658.
[11] F.K. Perkins, C. Hwang, M. Onllion, Y.-G. Kim, P.A. Dowben, Thin Solid Films 198 (1991) 317.
[12] R. Cheng, C.N. Borca, P.A. Dowben, Mat. Res. Soc. Symp. Proc. 614 (2000) F10.4.1.
[13] R. Cheng, C.N. Borca, P.A. Dowben, S. Stadler, Y.U. Idzerda, Appl. Phys. Lett. 78 (2001) 521.
[14] M. Rothschild, in: D.J. Ehrlich, J.Y. Tsao (Eds.), Laser Microfabrication: Thin Film Processes and Lithography, Academic Press, Boston, 1989, p. 163.
[15] P.M. Sousa, A.J. Silvestre, N. Popovici, M.L. Paramês, O. Conde, Mater. Sci. Forum 455–456 (2004) 20.
[16] T. Yu, Z.X. Shen, J. He, W.X. Sun, S.H. Tang, J.Y. Lin, J. Appl. Phys. 93 (2003) 3951.
[17] K.A. Singmaster, F.A. Houle, R.J. Wilson, Appl. Phys. Lett. 53 (1988) 1048.
[18] P. Hess, Spectrochim. Acta A 46 (1990) 489.
[19] T. Ivanova, M. Surtchev, K. Gesheva, Phys. Status Solidi 184 (2001) 507.
[20] G.W. Tyndall, R.L. Jackson, J. Chem. Phys. 91 (1989) 2881.
[21] G.W. Tyndall, R.L. Jackson, J. Am. Chem. Soc. 109 (1987) 582.
[22] J. Zuo, C. Xu, B. Hou, C. Wang, Y. Xie, Y. Qian, J. Raman Spectrosc. 27 (1996) 921.
[23] M.N. Iliev, A.P. Litvinchuk, H.-G. Lee, C.W. Chu, A. Barry, J.M.D. Coey, Phys. Rev. B 60 (1999) 33.